I_2-II-IV-VI_4 (I = Cu, Ag; II = Sr, Ba; IV = Ge, Sn; VI = S, Se): Chalcogenides for Thin Film Photovoltaics

Supporting Information

Tong Zhu[1], William P. Huhn[1], Garrett C. Wessler[1], Donghyeop Shin[1,2], Bayrammurad Saparov[3], David B. Mitzi[1,2], and Volker Blum[1,2]

[1]Department of Mechanical Engineering and Materials Science and [2]Department of Chemistry, Duke University, Durham, North Carolina 27708, United States
[3]Department of Chemistry & Biochemistry, University of Oklahoma, Norman, Oklahoma 73019, United States

Table S1. Basis functions (radial functions and their radial extent) in the "tight" numerical settings of FHI-aims used for the hybrid DFT calculations for elements I, II, IV, VI in compounds I_2-II-IV-VI_4 (I = Cu, Ag; II = Sr, Ba; IV = Ge, Sn; VI = S, Se). The nomenclature follows the convention employed in reference[1]. "Radial extent" refers to the parameter r_{cut} in Eq. (9) of reference[1].

	I **Cu**	**II** **Sr**	**IV** **Ge**	**VI** **S**
Rad. extent(Å)	6.0	7.0	6.0	6.0
Minimal[a]	[Ar]+4*s*3*p*3*d*	[Kr]+5*s*4*p*3*d*	[Ar]+4*s*4*p*3*d*	[Ne]+3*s*3*p*
Tight[b]	Cu^{2+}(4*p*) H(4*f*, 7.4) H(3*s*, 2.6) H(3*d*, 5) H(5*g*, 10.4)	Sr^{2+}(4*d*) Sr^{2+}(5*p*) H(4*f*, 5.6) Sr^{2+}(5*s*) H(5*g*, 7.4)	H(2*p*, 1.4) H(3*d*, 4.3) H(4*f*, 7.4) H(3*s*, 3.4)	S^{2+}(3*d*) H(2*p*, 1.8) H(4*f*, 7) S^{2+}(3*s*) H(4*d*, 6.2) H(5*g*, 10.8)
	Ag	**Ba**	**Sn**	**Se**
Rad. extent(Å)	6.0	8.0	6.0	6.0
Minimal[a]	[Kr]+5*s*4*p*4*d*	[Xe]+6*s*5*p*4*d*	[Kr]+5*s*5*p*4*d*	[Ar]+4*s*4*p*3*d*
Tight[b]	Ag^{2+}(5*p*) H(4*f*, 7.6) H(3*s*, 2.6) H(5*g*, 9.8) H(4*d*, 8.4)	Ba^{2+}(5*p*) Ba^{2+}(4*f*) H(3*p*, 2.7) H(4*s*, 3.3) H(4*f*, 5.8) H(5*g*, 7.4)	H(2*p*, 1.3) H(3*d*, 3.7) H(4*f*, 7.4) Sn^{2+}(5*s*)	H(3*d*, 4.3) H(2*p*, 1.6) H(4*f*, 7.2) Se^{2+}(4s)

[a]Minimal: Occupied radial functions of self-consistent (PBE functional) spherical free atoms. Nomenclature: noble gas configuration of the core and quantum numbers of the additional valence radial functions.

[b]"H(*nl*, *z*)": a hydrogen-like basis function for the bare Coulomb potential *z*/*r*, including its radial and angular momentum quantum numbers, *n* and *l*. "X^{2+}(*nl*)": a *n*, *l* radial function of a doubly positive free ion of species X.

Table S2. Comparison between the experimentally determined structure (derived directly from Ref. 2 and then transferred to the standard primitive cell[3] for space group *Ama2* using AFLOW-online[4]) and the computationally predicted structure (full HSE06 relaxation of unit cell vectors and atomic coordinates) of $Cu_2SrSnSe_4$. The structures are described by way of the lattice vectors (in Å) and the cell-internal relative atomic coordinates (in units of the lattice vectors).

$Cu_2SrSnSe_4$ (Ama2)						
Lattice Vectors						
	Experimental determined structure			Full HSE06 relaxed structure		
a	(3.3475, -5.377, 0)			(3.3801, -5.4456, 0)		
b	(3.3475, 5.377, 0)			(3.3801, 5.4456, 0)		
c	(0, 0, 10.9676)			(0, 0, 11.0548)		
Relative atomic coordinates						
	Experimentally determined structure			Full HSE06 relaxed structure		
Atom	u_x	u_y	u_z	u_x	u_y	u_z
Sn	0.1904	0.4918	1/4	0.1928	0.4927	0.2500
Sn	0.4918	0.1904	3/4	0.4926	0.1928	0.7501
Sr	0.7487	0.7487	1/2	0.7498	0.7498	0.5001
Sr	0.7487	0.7487	0.0	0.7498	0.7498	0.0000
Se	0.8788	0.0710	1/4	0.8776	0.0742	0.2500
Se	0.0710	0.8788	3/4	0.0741	0.8776	0.7501
Se	0.5779	0.4623	1/4	0.5767	0.4602	0.2501
Se	0.4623	0.5779	3/4	0.4601	0.5767	0.7500
Se	0.2418	0.7608	0.4298	0.2435	0.7608	0.4302
Se	0.7608	0.2418	0.5702	0.7607	0.2435	0.5700
Se	0.2418	0.7608	0.0702	0.2436	0.7609	0.0701
Se	0.7608	0.2418	0.9298	0.7608	0.2436	0.9301
Cu	0.5660	0.1298	0.3696	0.5682	0.1276	0.3691
Cu	0.1298	0.5660	0.6304	0.1274	0.5681	0.6310
Cu	0.5660	0.1298	0.1304	0.5684	0.1276	0.1310
Cu	0.1298	0.5660	0.8696	0.1275	0.5683	0.8691

Table S3. The relative fraction (in %) of the partial DOS for each chemical element near the valence and conduction band edges of the 16 compounds I_2-II-IV-VI_4 (I = Cu, Ag; II = Sr, Ba; IV = Ge, Sn; VI = S, Se) investigated in this work. The relative fraction (in %) is calculated based on the integrated areas of the partial DOS within 0.3 eV of either side of the VBM and CBM, i.e., the energy ranges shown in Figure 4 of the main paper. Thus, the relative fraction = (element partial DOS area) / (total DOS area). The area is obtained by integrating the area under the DOS curve based on trapezoidal rule for the domains [VBM−0.3 eV; VBM] / [CBM; CBM+0.3 eV] for valence/conduction band edges, respectively, discretized into 10 equally spaced steps. "Average" denotes the averaged fraction for the structures corresponding to each space group.

		Valence Band (VB) edge				**Conduction Band (CB) edge**			
Space Group	Compounds	Element				Element			
		VI	IV	I	II	VI	IV	I	II
$I\bar{4}2m$	Ag_2BaGeS_4	70%	1%	29%	0%	13%	10%	63%	14%
	Average	70%	1%	29%	0%	13%	10%	63%	14%
I222	Ag_2SrGeS_4	70%	1%	29%	0%	16%	11%	54%	19%
	$Ag_2BaGeSe_4$	73%	1%	26%	0%	22%	12%	46%	20%
	Ag_2BaSnS_4	67%	2%	31%	0%	22%	18%	35%	25%
	$Ag_2BaSnSe_4$	71%	2%	27%	0%	28%	17%	30%	25%
	$Ag_2SrGeSe_4$	73%	2%	25%	0%	22%	13%	46%	19%
	Ag_2SrSnS_4	67%	2%	31%	0%	24%	19%	36%	21%
	$Ag_2SrSnSe_4$	71%	1%	28%	0%	29%	19%	32%	20%
	Average	70%	2%	28%	0%	23%	16%	40%	21%
$P3_1$	Cu_2BaSnS_4	56%	3%	40%	1%	30%	27%	22%	21%
	Cu_2BaGeS_4	55%	3%	40%	2%	51%	20%	15%	14%
	$Cu_2BaGeSe_4$	64%	4%	30%	2%	38%	19%	28%	15%
	Cu_2SrSnS_4	55%	3%	41%	1%	29%	29%	20%	22%
	Average	58%	3%	38%	1%	37%	24%	21%	18%
$P3_2$	Cu_2SrGeS_4	56%	3%	40%	1%	53%	20%	13%	14%
	Average	56%	3%	40%	1%	53%	20%	13%	14%
Ama2	$Cu_2BaSnSe_4$	66%	3%	30%	1%	37%	27%	17%	19%
	$Cu_2SrGeSe_4$	60%	2%	36%	2%	57%	19%	11%	13%
	$Cu_2SrSnSe_4$	62%	3%	33%	2%	34%	27%	19%	20%
	Average	63%	3%	32%	2%	43%	24%	16%	17%

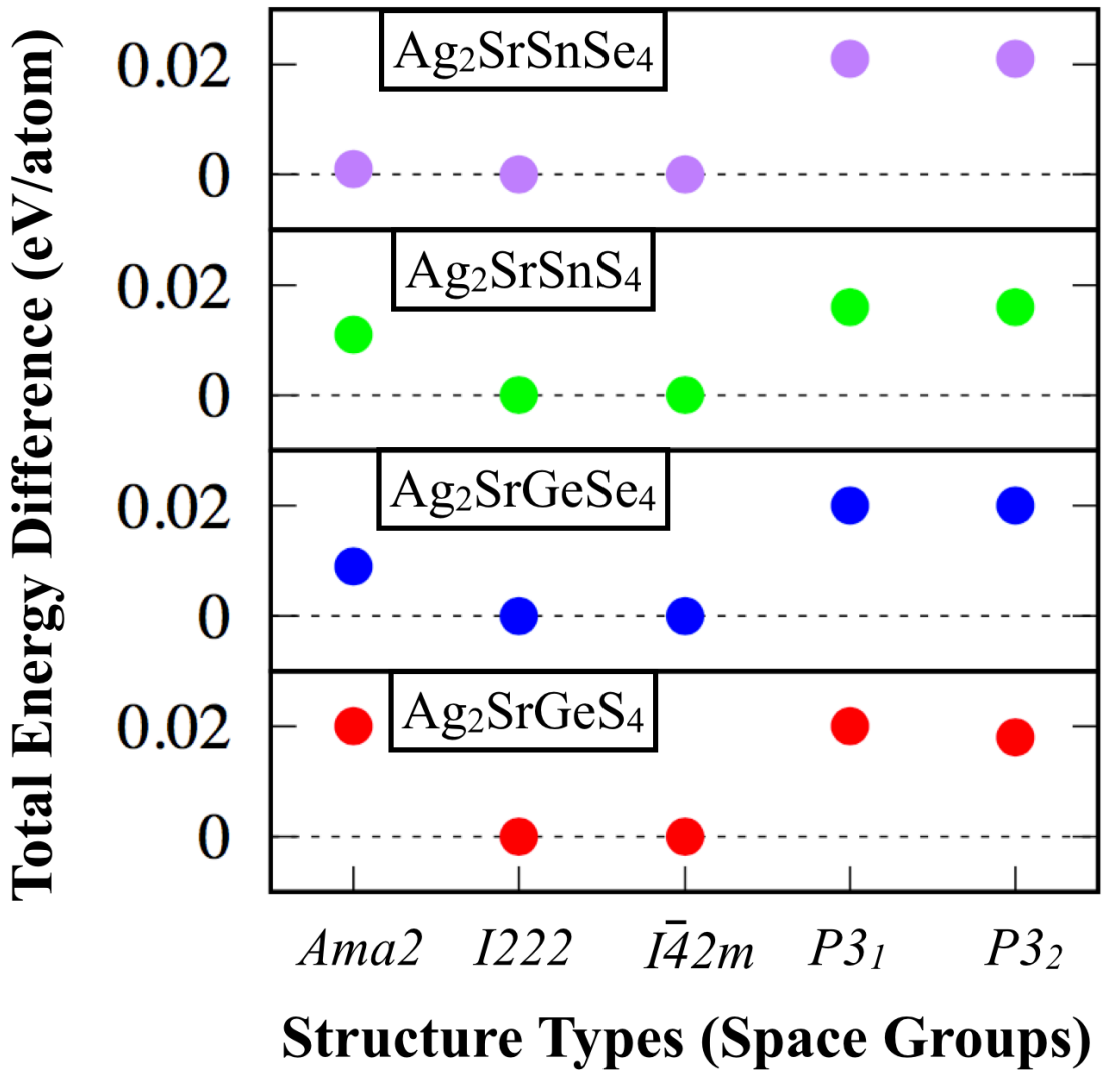

Figure S1. Total energy difference of five different prospective structure types (space groups: *Ama2*, *I222*, *I$\bar{4}$2m*, *P3$_1$*, *P3$_2$*) for four compounds (Ag_2SrGeS_4, Ag_2SrSnS_4, $Ag_2SrSnSe_4$, $Ag_2SrGeSe_4$, shown as red, green, purple, and blue circles, respectively), for which no experimental crystal structure is known. The total energies are calculated by DFT-HSE06 based on fully HSE06-relaxed geometries. The total energy of the lowest-energy structure among these five different structure types for each compound is chosen as the reference value (0 eV/atom). Since the structure pairs *I222*/ *I$\bar{4}$2m* and *P3$_1$*/*P3$_2$* are closely related (as subgroups and enantiomorphic groups, respectively), the formation energies of these structure pairs are almost the same for full structure optimizations at the HSE06 theory level.

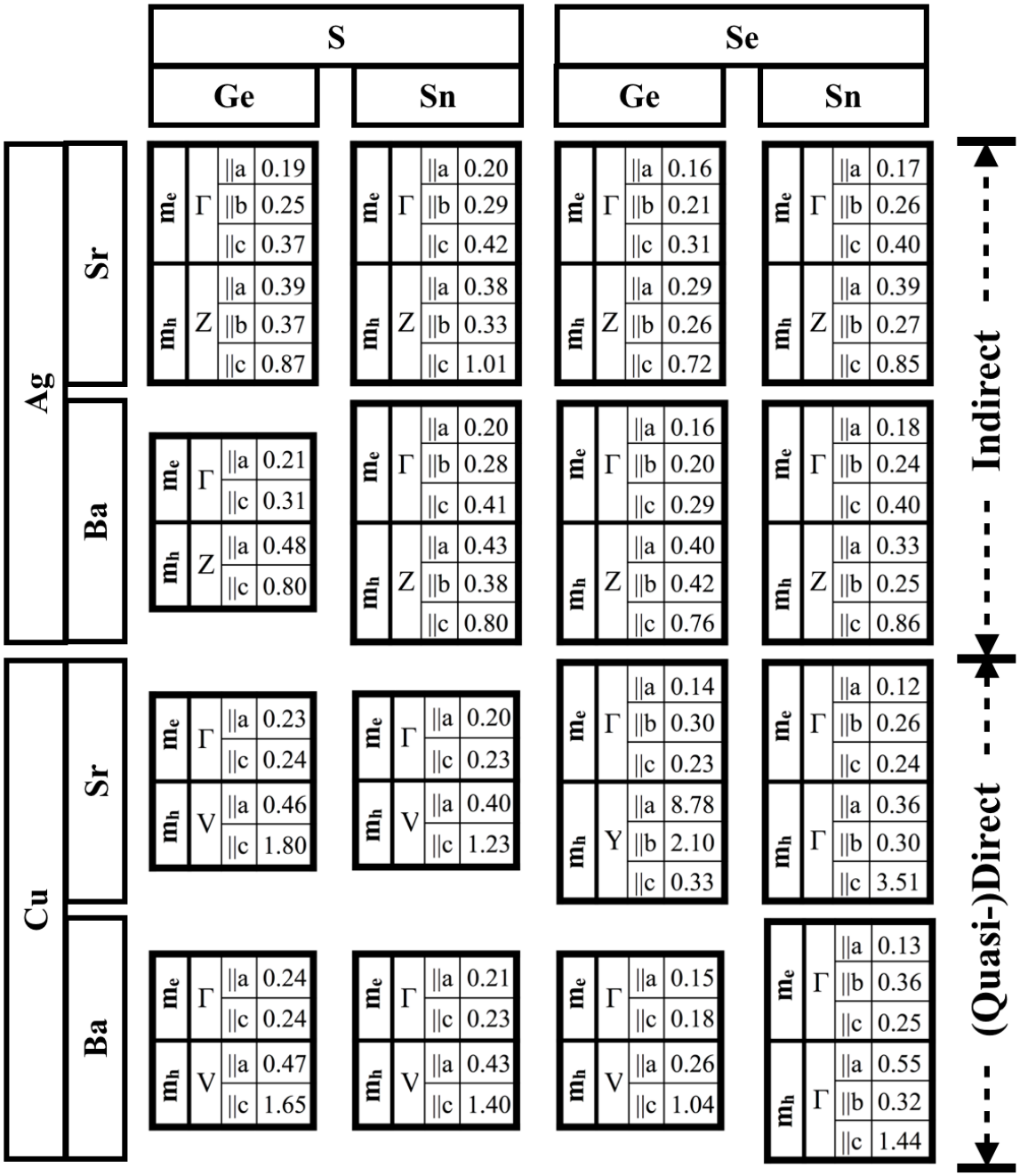

Figure S2. Numerical values and k-space directions of the effective mass tensors of electrons (m_e) and holes (m_h) shown in Figure 5 of the main paper. Effective masses were determined by parabolic fits to the calculated band structures for the lowest conduction band and the highest valence band at the extremal k points for the 16 compounds studied here. The values are given in units of the free electron mass m_0. For compounds that belong to the tetragonal ($I\bar{4}2m$) and trigonal crystal ($P3_1$ and $P3_2$) structures, we only show the tensor values in two directions (||a and ||c) since the tensor value in the ||b direction is identical to that in the ||a direction.

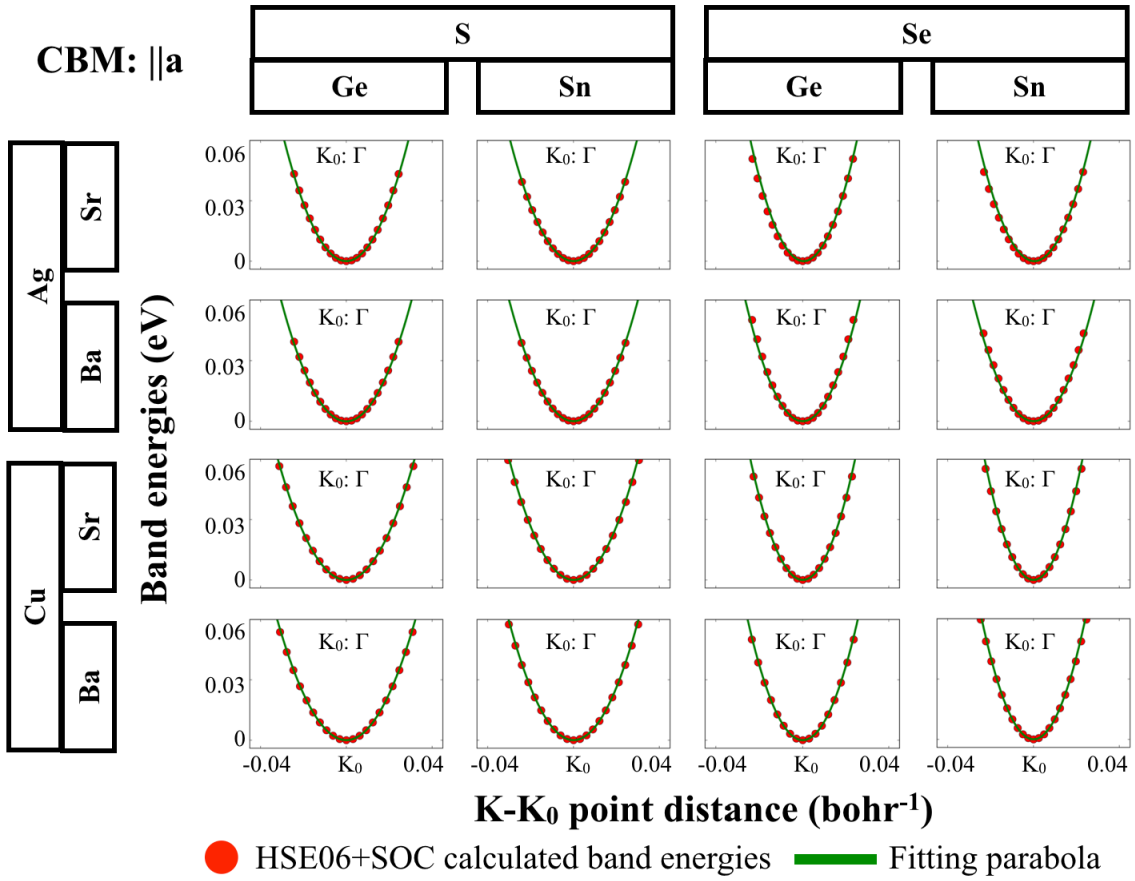

Figure S3. DFT-HSE06+SOC eigenvalues ε(K) ("band energies", red dots) and parabolic fits E(K) (continuous green curves) to a restricted data range to determine band curvatures and approximate effective masses of electrons (m_e) for the conduction band minimum (CBM) along reciprocal a axis directions (||a) in the conventional cell for the 16 compounds studied in this work. The elemental components of this 4×4 compound matrix appear along the left and top panels. The parabolic fits to the DFT data were obtained within a fitting range $K_0 \pm 0.01$ bohr^{-1} around the crystal momentum k_0 associated with each CBM. Outside this range, the green curves shown are extrapolated for comparison with the actual DFT data. The y axes indicate the band energies, referenced to the CBM as the respective energy zeros. The x axes indicate the crystal momentum K-K_0 (in bohr^{-1}) in the ||a direction. The reference point K_0 is given in each plot and corresponds to the location of the CBM in reciprocal space as determined by earlier band structure calculations on a coarser k-space grid. The fit functions used to obtain the effective mass tensor values are shown as follows: $E(K) = E_{VBM/CBM} + \hbar^2(K\text{-}K_0)^2/2m^*$. For the CBM effective mass tensor along the ||a direction, we fixed the *k* point (K_0) and band energy value ($E_{VBM/CBM}$) corresponding to the VBM/CBM. The resulting effective mass parameters for each parabolic fit are shown in Figure 5.

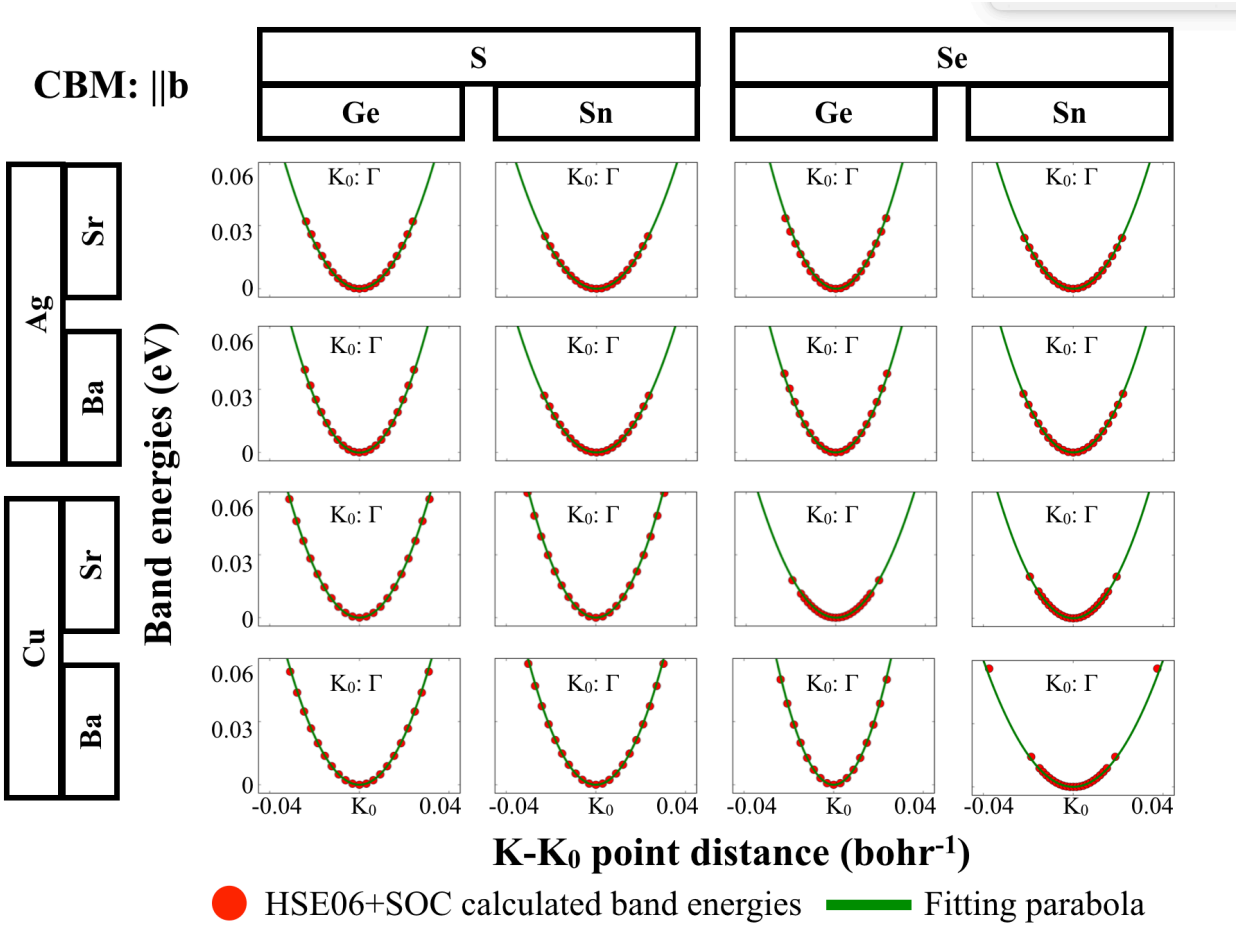

Figure S4. DFT-HSE06+SOC eigenvalues ε(K) ("band energies", red dots) and parabolic fits E(K) (continuous green curves) to a restricted data range to determine band curvatures and approximate effective masses of electrons (m_e) for the conduction band minimum (CBM) along reciprocal b axis directions (||b) in the conventional cell for the 16 compounds studied in this work. For other details, see the caption of Figure S3.

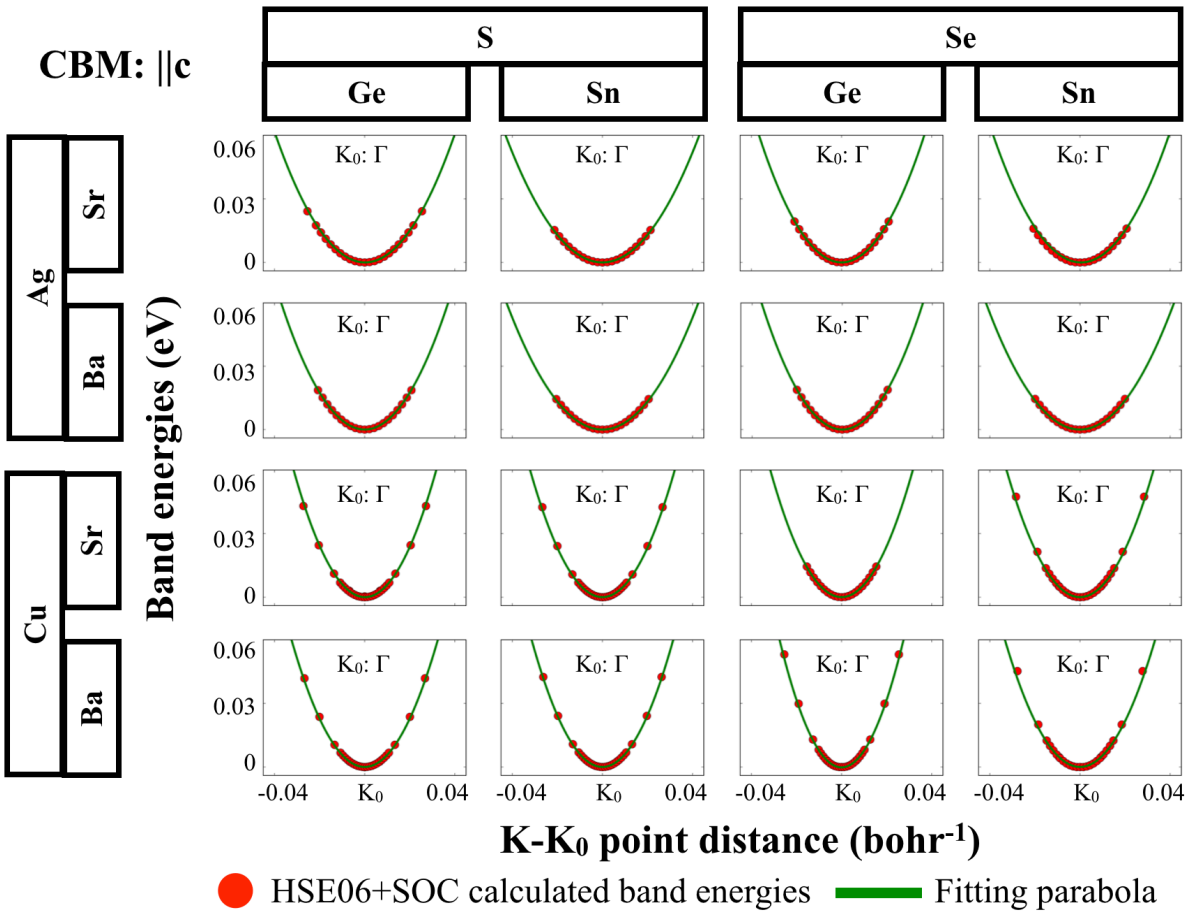

Figure S5. DFT-HSE06+SOC eigenvalues ε(K) ("band energies", red dots) and parabolic fits E(K) (continuous green curves) to a restricted data range to determine band curvatures and approximate effective masses of electrons (m_e) for the conduction band minimum (CBM) along the reciprocal c axis directions (||c) in the conventional cell for the 16 compounds studied in this work. For other details, see the caption of Figure S3.

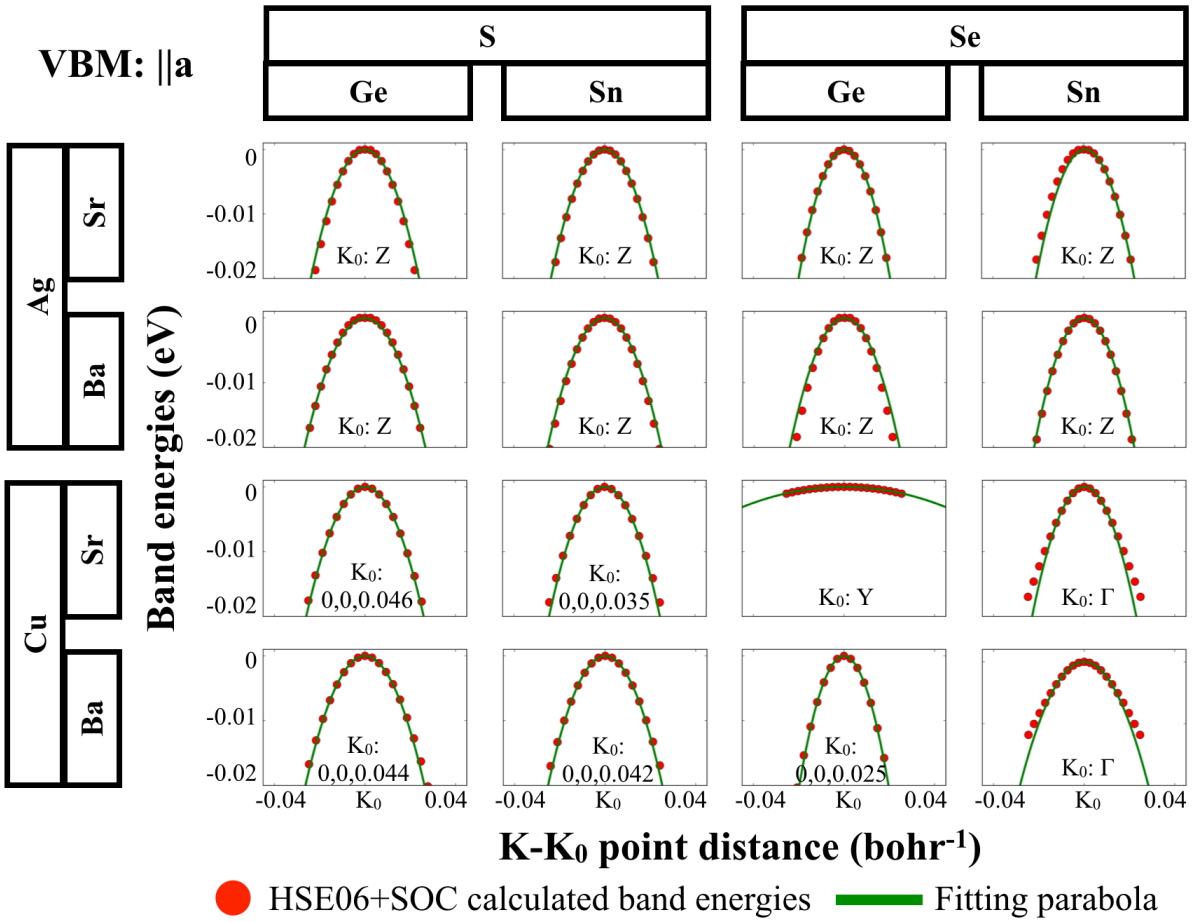

Figure S6. DFT-HSE06+SOC eigenvalues ε(K) ("band energies", red dots) and parabolic fits E(K) (continuous green curves) to a restricted data range to determine band curvatures and approximate effective masses of holes (m_h) for the valence band maximum (VBM) along the reciprocal a axis directions (||a) in the conventional cell for the 16 compounds studied in this work. For other details, see the caption of Figure S3.

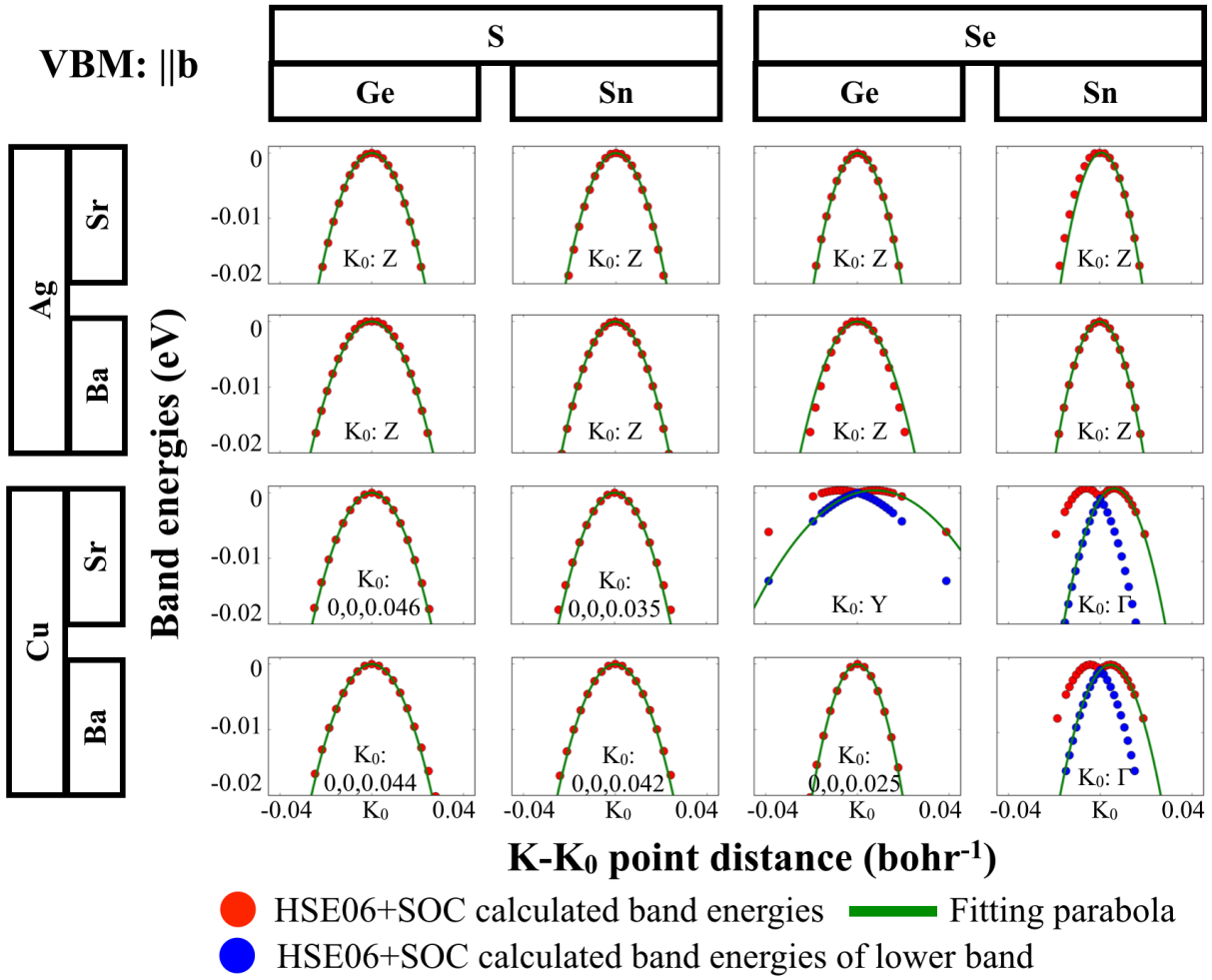

Figure S7. DFT-HSE06+SOC eigenvalues ε(K) ("band energies", red dots) and parabolic fits E(K) (continuous green curves) to a restricted data range to determine band curvatures and approximate effective masses of holes (m_h) for the valence band maximum (VBM) along reciprocal b axis directions (||b) in the conventional cell for the 16 compounds studied in this work. For other details, see the caption of Figure S3. We note that the VBMs of some compounds ($Cu_2SrGeSe_4$, $Cu_2SrSnSe_4$, $Cu_2BaSnSe_4$) are split and slightly off-K_0 in the ||b direction. In these cases, we let the fit procedure find the actual VBM energies and corresponding k-points k_0. In order to check the extrapolated fitting curve, the DFT-HSE06+SOC eigenvalues ε(k) of the split counterpart of each band are also shown as blue symbols for those structures. The extrapolated fit curves are exactly the same as those lower band energies (blue dots) and reveal band crossings among the split, slightly off-K_0 bands.

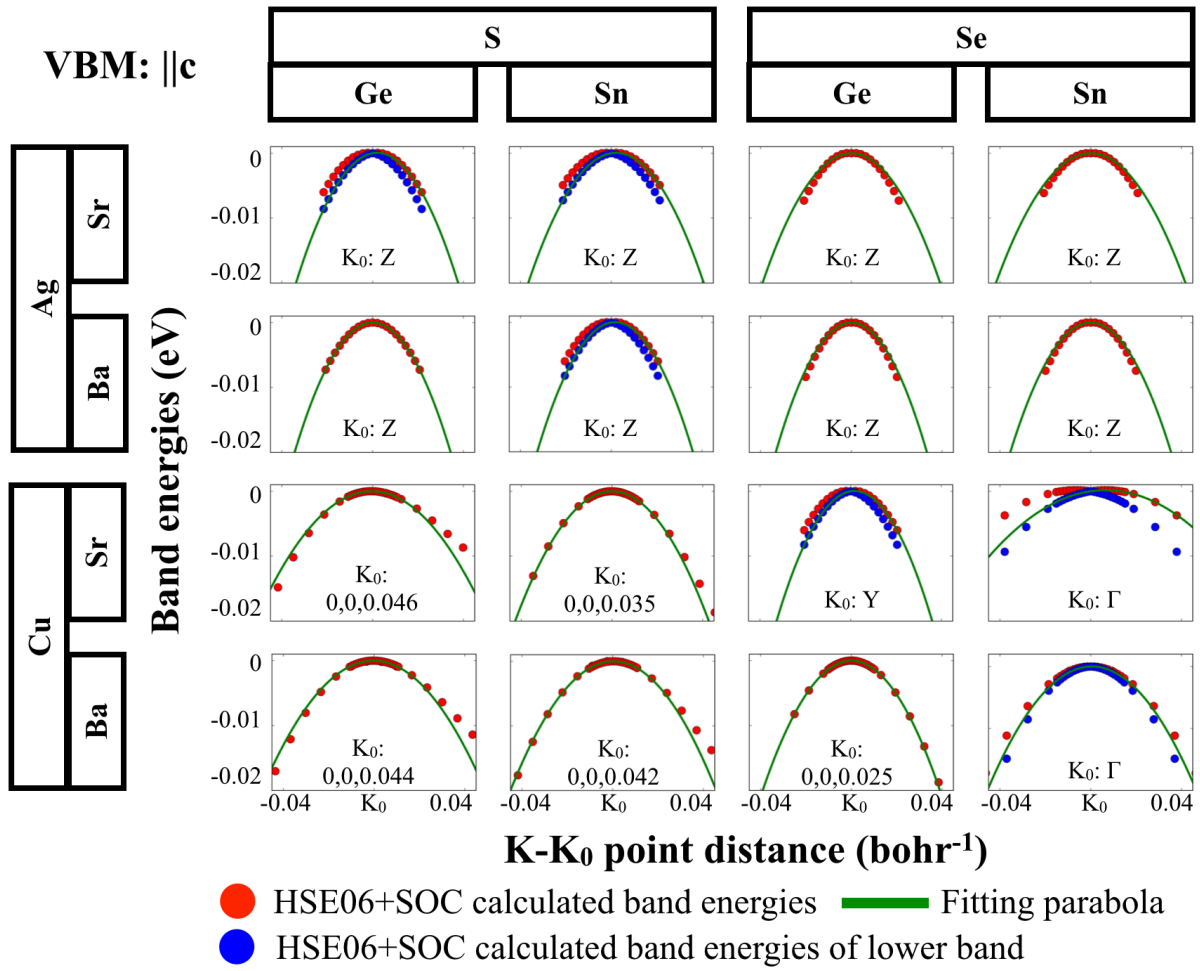

Figure S8. DFT-HSE06+SOC eigenvalues ε(K) ("band energies", red dots) and parabolic fits E(K) (continuous green curves) to a restricted data range to determine band curvatures and approximate effective masses of holes (m_h) for the valence band maximum (VBM) along reciprocal c axis directions (||c) in the conventional cell for the 16 compounds studied in this work. For other details, see the caption of Figure S3. As in Fig. S7, the VBMs of some compounds in the ||c direction are also split and slightly off-K_0. They are graphed and treated as described in the caption of Fig. S7.

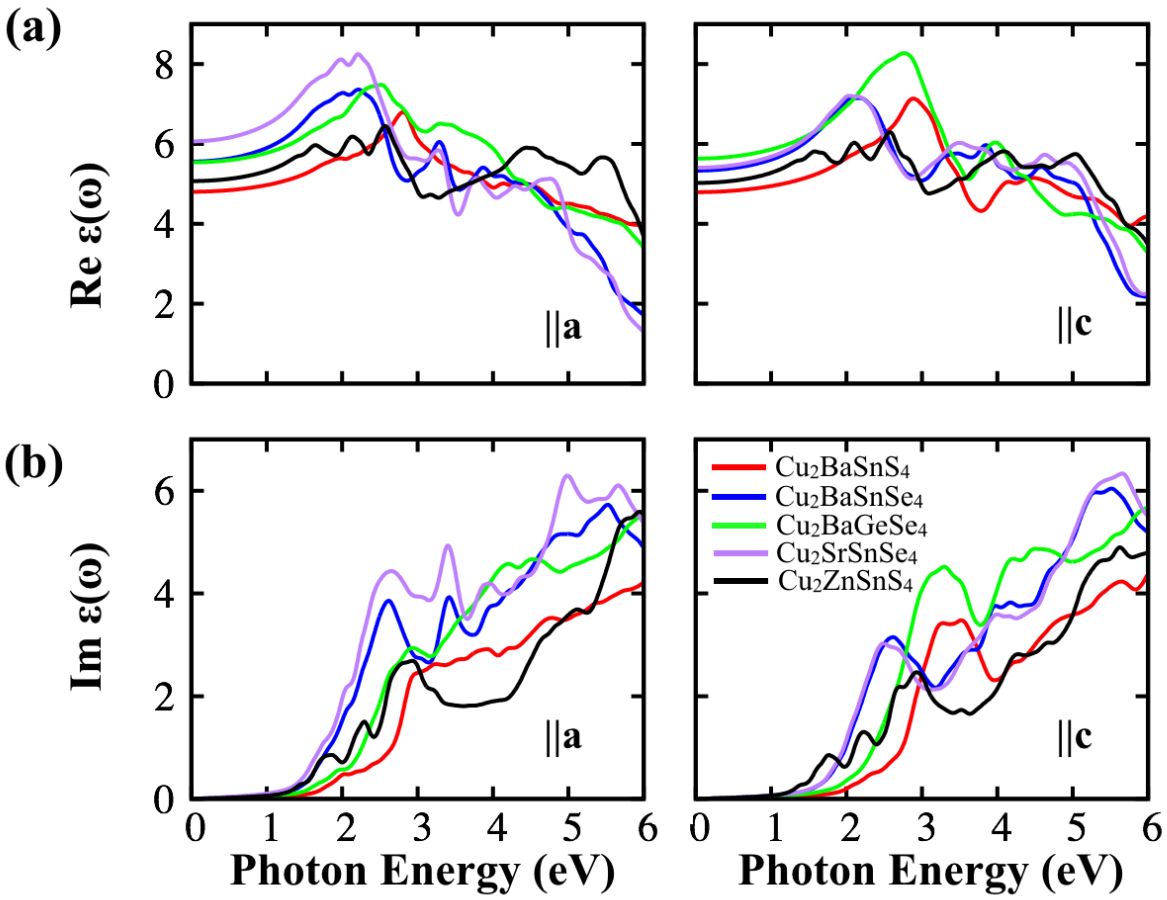

Figure S9. The calculated real (a) and imaginary (b) parts of the dielectric function plotted in different directions (||a parallel to reciprocal a axis, ||c parallel to reciprocal c axis) for the four candidate compounds: $Cu_2BaGeSe_4$ (green lines), $Cu_2SrSnSe_4$ (purple lines), Cu_2BaSnS_4 (red lines), and $Cu_2BaSnSe_4$ (blue lines), using the standard HSE06 functional including spin-orbit coupling. Results for the kesterite compound $Cu_2ZnSnSe_4$ are also shown for comparison (black lines). The unit cell parameters and atomic coordinates of the hypothetical, fully ordered kesterite structure of $Cu_2ZnSnSe_4$ are derived from a structure optimization at the DFT-HSE06 level of theory.

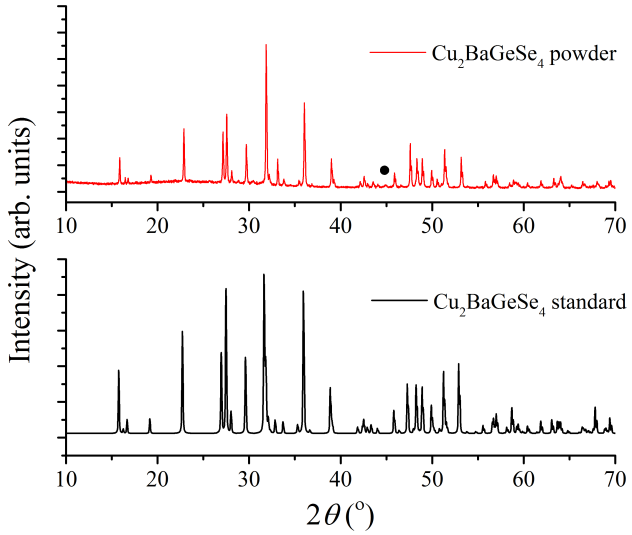

Figure S10. XRD patterns of (a) experimentally-prepared $Cu_2BaGeSe_4$ powder and (b) the standard $Cu_2BaGeSe_4$ pattern[5]. A very weak unidentified (presumably an impurity phase) peak is labelled with a filled circle.

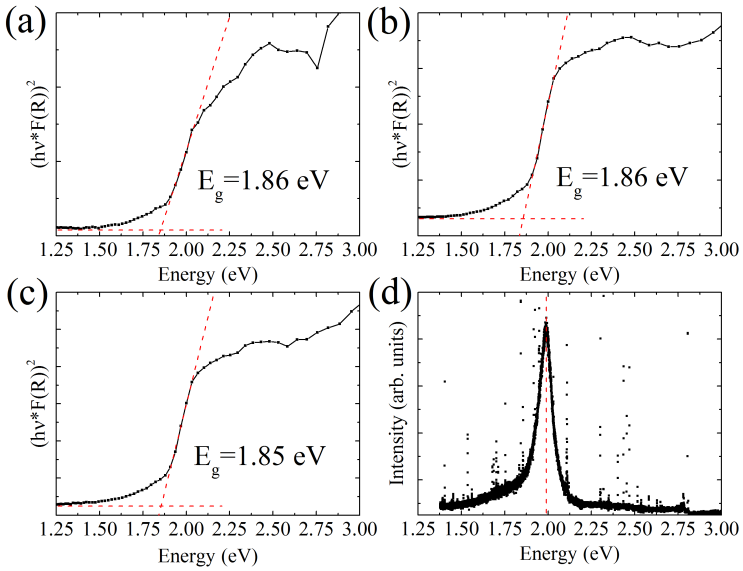

Figure S11. Diffuse reflectance plots of $Cu_2BaGeSe_4$ powder, diluted in $BaSO_4$ at concentrations of (a) 5%, (b) 10%, and (c) 20%. Red lines are linear fits of the absorption edge corresponding to direct band gaps of 1.86(5) eV for each of the diluted samples. Photoluminescence spectrum of undiluted $Cu_2BaGeSe_4$ powder under 442 nm excitation laser (d).

Supplementary Experimental Procedure and Analysis

To prepare powder of $Cu_2BaGeSe_4$, stoichiometric mixtures of BaSe (Materion, 99.5%), CuSe (Alfa Aesar, 99.5%), Ge (Alfa Aesar, 99.999%), and Se (Alfa Aesar, 99.999%) were

ground and cold-pressed into pellets. The BaSe and CuSe starting materials were baked on a hotplate prior to use at 175°C, in a N_2 filled glovebox, to remove SeO_2 impurities within the powders. These pellets were transferred to quartz ampoules (pre-baked and evacuated to ~1×10^{-6} torr) and flame-sealed under dynamic vacuum. Before sealing, a small amount of excess Se powder (~2.5 mg) was inserted into the ampoules with the 167.3 mg $Cu_2BaGeSe_4$ precursor pellet to create an overpressure of Se vapor and avoid oxide formation. The ampoules were then heated to 650°C in a box furnace at a rate of 100°C/hr and held at this temperature for 24 hours. The steps of grinding, homogenizing, cold-pressing, and annealing the pellets were repeated several times to ensure a homogeneous powder. In order to evaluate the crystal structure of the samples, powder X-ray diffraction (PXRD) patterns were measured using a PANalytical Empyrean with Cu-Kα radiation under ambient conditions. The initial PXRD data showed that the dominant phase was $Cu_2BaGeSe_4$ with small amounts of impurity phases such as SeO_2, GeO_2, and $CuSeO_3$. Finally, the ground powder after several pellet annealing treatments was baked at 175°C on a hot plate in a N_2-filled glovebox to reduce the remaining oxide phases. A PXRD pattern of a sample after this step is show in Figure S10.

To determine the band gap of the bulk samples, diffuse reflectance measurements were performed on powder samples using an Enlitech QE-R Quantum Efficiency/Reflectivity system. A $Cu_2BaGeSe_4$ sample was diluted at various concentrations (5, 10, 20%) in $BaSO_4$ to evaluate the effect of the dilution on the measured band gap. The diffuse reflectance measurements yield a direct band gap of 1.86(5) eV for the diluted samples, which agrees well with the 1.91(5) value from the undiluted sample. Photoluminescence measurements were taken using a Horiba Jobin Yvon LabRam ARAMIS system using a 442 nm HeCd excitation laser. This measurement yields an emission maximum at 1.98(1) eV. This value is within 70 meV of the band gap measured by diffuse reflectance (undiluted sample).

Comparative calculated HSE06 band structures without spin-orbit coupling for five compounds

To illustrate the impact of spin-orbit coupling on the overall band structures of the compounds considered here, we recomputed the band structures of the five compounds $Cu_2BaGeSe_4$, $Cu_2BaSnSe_4$, $Cu_2SrGeSe_4$, $Cu_2SrSnSe_4$, and $Ag_2BaSnSe_4$ *without* including SOC effects. The selected Cu-containing compounds are all Se based and are thus expected to show larger SOC effects than their lighter S-based counterparts. Additionally, three of the four potentially most interesting compounds for PV in this work are included among them ($Cu_2BaGeSe_4$, $Cu_2BaSnSe_4$, $Cu_2SrSnSe_4$). The $Ag_2BaSnSe_4$ compound reflects the overall heaviest combination of elements studied in this work and is thus selected as a representative Ag-based compound with the largest expected SOC effect. Figures S12-S16 show comparisons of band structures of all five compounds without and with SOC effects, as well as band curvature plots near the VBM and CBM for comparison to their SOC-including counterparts in Figs. S3-S8.

SOC effects arise most prominently in the valence band at the Γ point (other bands may appear shifted since the band energy zero is chosen to be the VBM). The predicted band gaps for the five compounds thus vary most if the VBM is located at Γ, summarized below:

$Cu_2BaGeSe_4$	E_g (no SOC) = 1.66 eV	E_g (SOC) = 1.60 eV
$Cu_2BaSnSe_4$	E_g (no SOC) = 1.57 eV	E_g (SOC) = 1.50 eV
$Cu_2SrGeSe_4$	E_g (no SOC) = 1.80 eV	E_g (SOC) = 1.79 eV
$Cu_2SrSnSe_4$	E_g (no SOC) = 1.51 eV	E_g (SOC) = 1.46 eV
$Ag_2BaSnSe_4$	E_g (no SOC) = 0.78 eV	E_g (SOC) = 0.77 eV

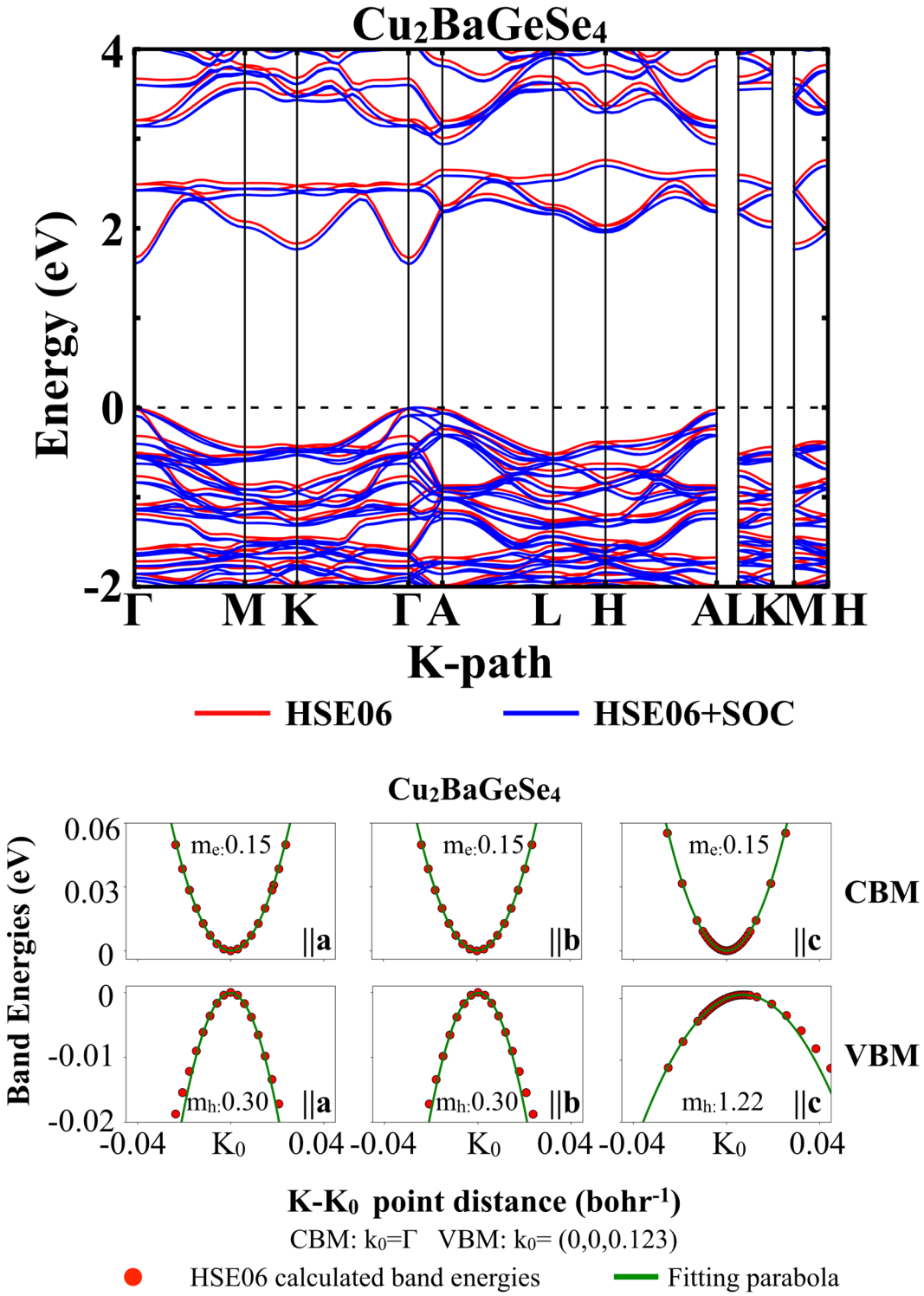

Figure S12. Top: Comparison of calculated band structures without (red) vs. with (blue) SOC effects for the $Cu_2BaGeSe_4$ compound (*P3₁* space group). Bottom: Close-up view of the band curvatures and fitted effective masses in three reciprocal-space directions at the VBM and CBM without including SOC effects. For analogous close-up views of the band curvatures and fitted effective masses with SOC included, see Figs S3-S8.

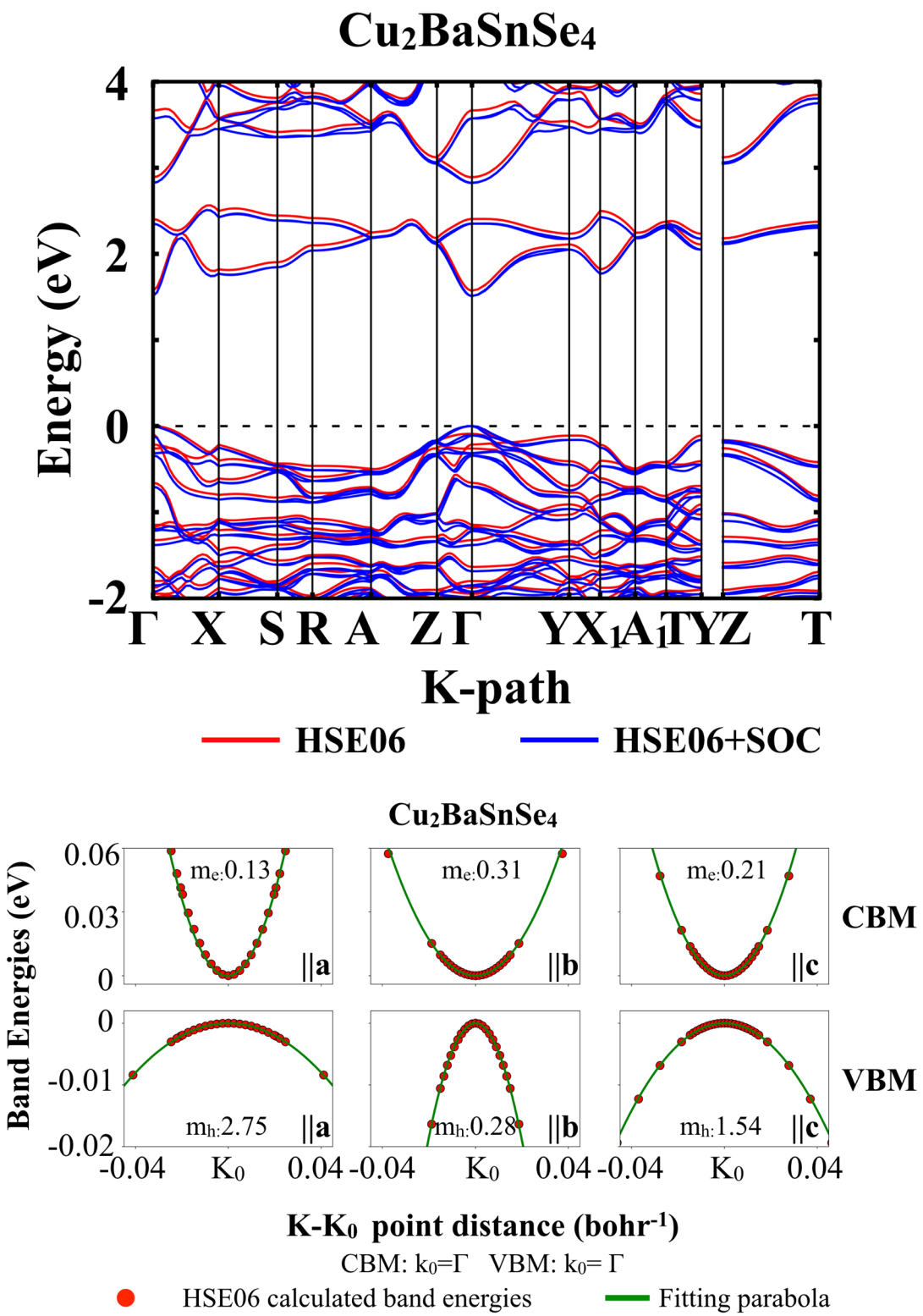

Figure S13. Top: Comparison of calculated band structures without (red) vs. with (blue) SOC effects for the $Cu_2BaSnSe_4$ compound (*Ama2* space group). Bottom: Close-up view of the band curvatures and fitted effective masses in three reciprocal-space directions at the VBM and CBM without including SOC effects. For analogous close-up views of the band curvatures and fitted effective masses with SOC included, see Figs S3-S8.

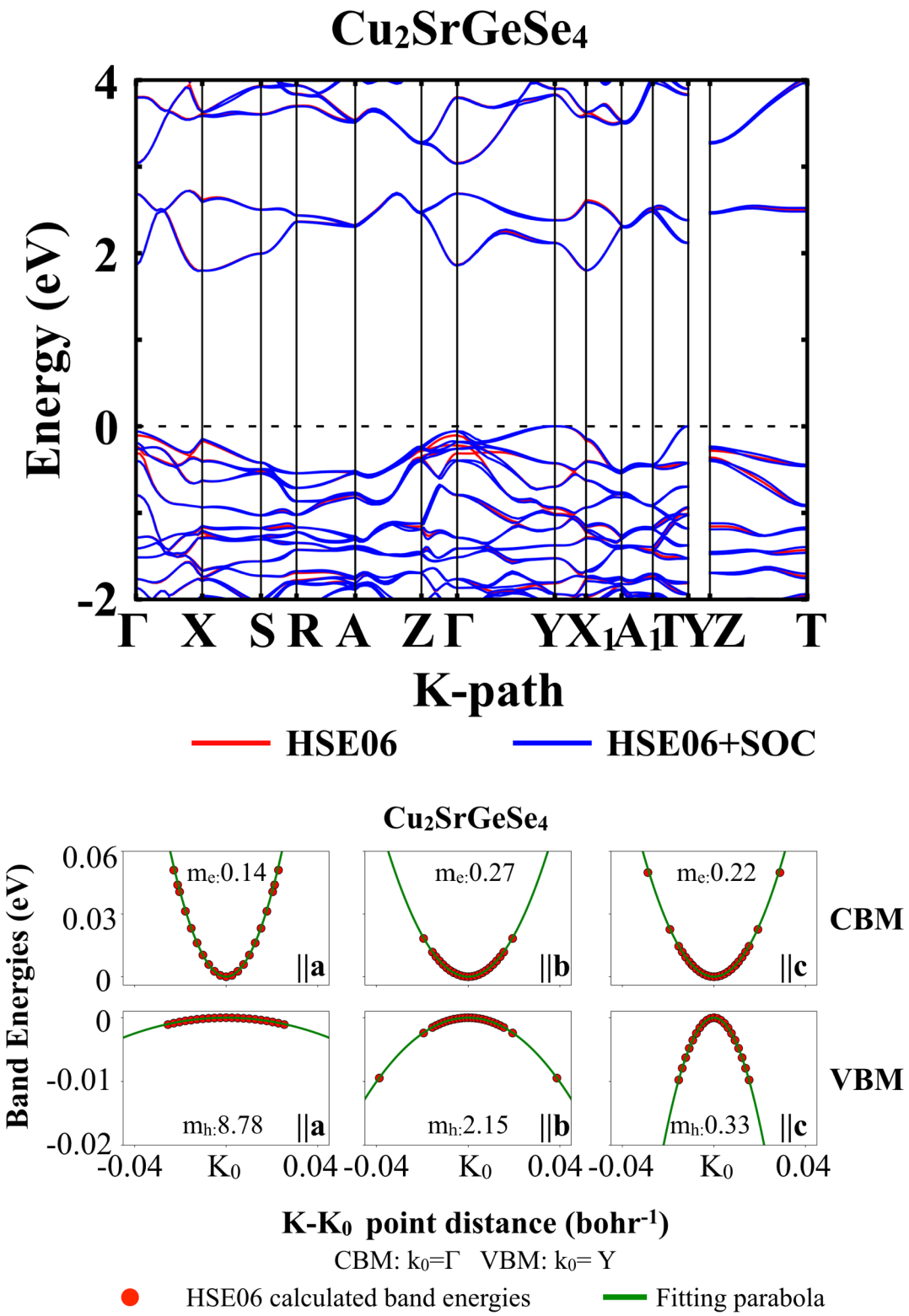

Figure S14. Top: Comparison of calculated band structures without (red) vs. with (blue) SOC effects for the $Cu_2SrGeSe_4$ compound (*Ama2* space group). Bottom: Close-up view of the band curvatures and fitted effective masses in three reciprocal-space directions at the VBM and CBM without including SOC effects. For analogous close-up views of the band curvatures and fitted effective masses with SOC included, see Figs S3-S8.

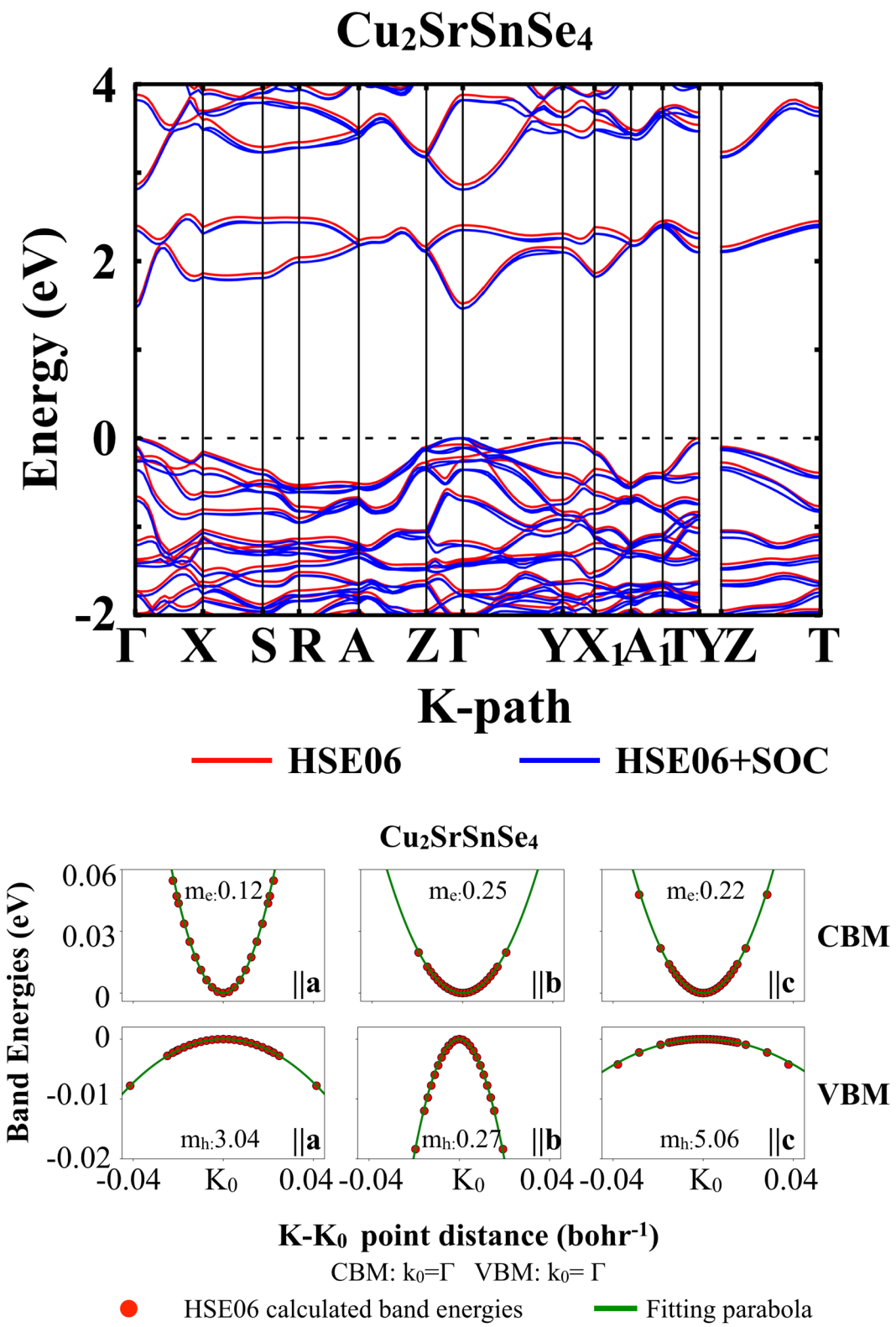

Figure S15. Top: Comparison of calculated band structures without (red) vs. with (blue) SOC effects for the $Cu_2SrSnSe_4$ compound (*Ama2* space group). Bottom: Close-up view of the band curvatures and fitted effective masses in three reciprocal-space directions at the VBM and CBM without including SOC effects. For analogous close-up views of the band curvatures and fitted effective masses with SOC included, see Figs S3-S8.

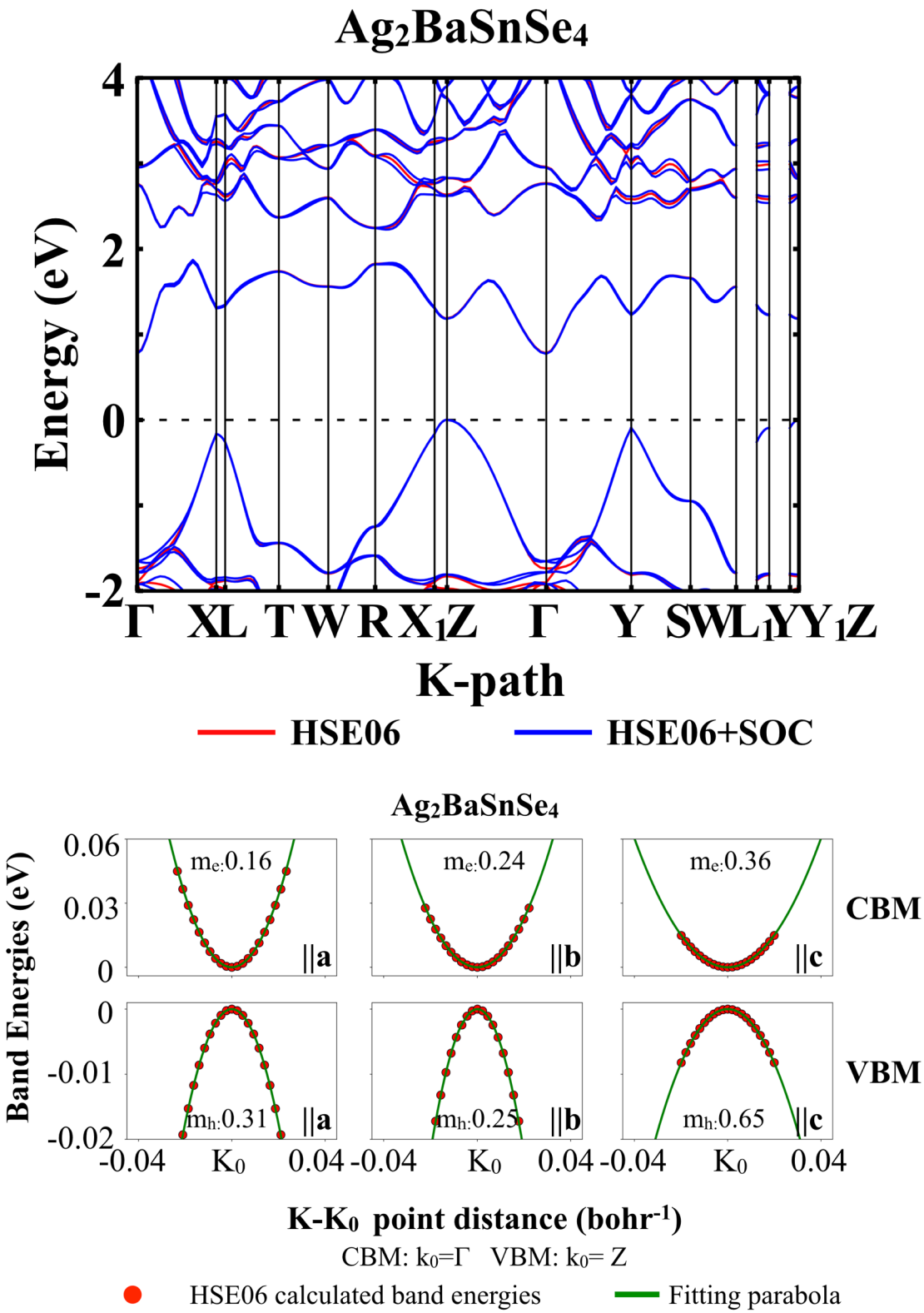

Figure S16. Top: Comparison of calculated band structures without (red) vs. with (blue) SOC effects for the $Ag_2BaSnSe_4$ compound (*I222* space group). Bottom: Close-up view of the band curvatures and fitted effective masses in three reciprocal-space directions at the VBM and CBM without including SOC effects. For analogous close-up views of the band curvatures and fitted effective masses with SOC included, see Figs S3-S8.

Geometry Information for Electronic Structure Calculations

The following section provides the unit cell parameters and cell-internal atomic coordinates used in the electronic structure analysis for the 16 compounds I_2-II-IV-VI_4 (I = Cu, Ag; II = Sr, Ba; IV = Ge, Sn; VI = S, Se) considered in this work, as well as the structure used for the comparison to Cu_2ZnSnS_4, in FHI-aims' geometry format. The specific relaxation strategy used is described in the bracket under each compound name. The corresponding space groups are also listed in the bracket. Lattice vectors are given in Å, while atomic coordinates are given in fractional units of the three lattice vectors. FHI-aims' geometry format can be read by standard viewing programs (e.g., jmol) and can be converted into other formats using OpenBabel.

Ag_2SrGeS_4 (*I222*)

(Full HSE06 relaxation geometry based on "tight" basis sets for the lowest-energy structure among 5 space group: *I222, $I\bar{4}2m$, $P3_1$, $P3_2$, Ama2*)

```
lattice_vector  -3.41008064663983   3.48674450693820   3.84528746647537
lattice_vector   3.41008064663983  -3.48674450693820   3.84528746647537
lattice_vector   3.41008064663983   3.48674450693820  -3.84528746647537
atom_frac   0.00000000000000   0.00000000000000   0.00000000000000  Sr
atom_frac   0.50026037000000   0.50026037000000   0.00000000000000  Ge
atom_frac   0.71236839000000   0.21166493000000   0.50070346000000  Ag
atom_frac   0.28947266000000   0.78883967000000   0.50063299000000  Ag
atom_frac   0.15087285000000   0.14738972000000   0.62619878000000  S
atom_frac   0.52165359000000   0.52384021000000   0.37348549000000  S
atom_frac   0.85093269000000   0.47668162000000   0.99705545000000  S
atom_frac   0.48012829000000   0.85312452000000   0.00269878000000  S
```

Ag_2BaGeS_4 (*$I\bar{4}2m$*)

(Fixed experimental lattice constants with atomic coordinates relaxed by HSE06 based on "tight" basis sets)

```
lattice_vector  -3.41400000000000   3.41400000000000   4.00850000000000
lattice_vector   3.41400000000000  -3.41400000000000   4.00850000000000
lattice_vector   3.41400000000000   3.41400000000000  -4.00850000000000
atom_frac    0.50000022000000   0.50000003000000   0.00000000000000  Ba
atom_frac    0.74999979000000   0.24999977000000   0.50000001000000  Ag
atom_frac    0.25000009000000   0.75000015000000   0.49999986000000  Ag
atom_frac    0.00000000000000   0.00000000000000   0.00000000000000  Ge
atom_frac    0.96677191000000   0.96677149000000   0.62191145000000  S
atom_frac    0.03322850000000   0.65514006000000   0.00000000000000  S
atom_frac    0.34485996000000   0.34486052000000   0.37808839000000  S
atom_frac    0.65513956000000   0.03322795000000   0.00000000000000  S
```

Ag_2SrSnS_4 (*I222*)

(Full HSE06 relaxation geometry based on "tight" basis sets for the lowest-energy structures among 5 space group: *I222, $I\bar{4}2m$, $P3_1$, $P3_2$, Ama2*)

```
lattice_vector  -3.45526614138827   3.61681200684263   3.89935405950391
lattice_vector   3.45526614138827  -3.61681200684263   3.89935405950391
lattice_vector   3.45526614138827   3.61681200684263  -3.89935405950391
atom_frac   0.00155029000000   0.00000000000000   0.00155029000000  Sr
atom_frac   0.50085671000000   0.49954399000000   0.00131272000000  Sn
atom_frac   0.30053936000000   0.79945350000000   0.50108586000000  Ag
atom_frac   0.70113338000000   0.19982084000000   0.50131254000000  Ag
atom_frac   0.49160227000000   0.87985123000000   0.01297531000000  S
atom_frac   0.86974889000000   0.47755181000000   0.98976654000000  S
atom_frac   0.51149871000000   0.52159842000000   0.39190884000000  S
atom_frac   0.13291026000000   0.11936307000000   0.61091732000000  S
```

Ag_2BaSnS_4 (*I222*)
(Fixed experimental lattice constants with atomic coordinates relaxed by HSE06 based on "tight" basis sets)

```
lattice_vector  -3.42700000000000   3.56350000000000   4.05850000000000
lattice_vector   3.42700000000000  -3.56350000000000   4.05850000000000
lattice_vector   3.42700000000000   3.56350000000000  -4.05850000000000
atom_frac   0.00000000000000   0.00000000000000   0.00000000000000  Ba
atom_frac   0.50000007000000   0.50000007000000   0.00000000000000  Sn
atom_frac   0.70075013000000   0.20075157000000   0.49999856000000  Ag
atom_frac   0.29924772000000   0.79924822000000   0.49999950000000  Ag
atom_frac   0.13599123000000   0.12891687000000   0.60337313000000  S
atom_frac   0.52553968000000   0.53261472000000   0.39662587000000  S
atom_frac   0.86401115000000   0.46738510000000   0.99292501000000  S
atom_frac   0.47445613000000   0.87108326000000   0.00707431000000  S
```

$Ag_2SrGeSe_4$ (*I222*)
(Full HSE06 relaxation geometry based on "tight" basis sets for the lowest-energy structures among 5 space group: *I222, $I\bar{4}2m$, $P3_1$, $P3_2$, Ama2*)

```
lattice_vector  -3.55760809750732   3.69485326707066   3.97579574077763
lattice_vector   3.55760809750732  -3.69485326707066   3.97579574077763
lattice_vector   3.55760809750732   3.69485326707066  -3.97579574077763
atom_frac   0.00143290000000   0.00312541000000   0.00000000000000  Sr
atom_frac   0.50142191000000   0.50310452000000   0.00000000000000  Ge
atom_frac   0.69926462000000   0.20118397000000   0.50078131000000  Ag
atom_frac   0.30313393000000   0.80517351000000   0.50077753000000  Ag
atom_frac   0.14427362000000   0.14149167000000   0.62219303000000  Se
atom_frac   0.51844069000000   0.52499298000000   0.37987162000000  Se
atom_frac   0.85846432000000   0.48108072000000   0.99616608000000  Se
atom_frac   0.48415168000000   0.86479971000000   0.00563031000000  Se
```

$Ag_2BaGeSe_4$ (*I222*)
(Fixed experimental lattice constants with atomic coordinates relaxed by HSE06 based on "tight" basis sets)

```
lattice_vector  -3.52900000000000   3.63150000000000   4.12650000000000
lattice_vector   3.52900000000000  -3.63150000000000   4.12650000000000
lattice_vector   3.52900000000000   3.63150000000000  -4.12650000000000
atom_frac   0.49996231000000   0.49998542000000   0.00000000000000  Ba
atom_frac   0.79574867000000   0.29561569000000   0.49997822000000  Ag
atom_frac   0.20436733000000   0.70438802000000   0.50000391000000  Ag
atom_frac   0.35301652000000   0.35375834000000   0.38406789000000  Se
atom_frac   0.03103063000000   0.64697766000000   0.00000000000000  Se
atom_frac   0.96968292000000   0.96896374000000   0.61595604000000  Se
atom_frac   0.64623149000000   0.03032887000000   0.00000000000000  Se
atom_frac   0.00000000000000   0.00000000000000   0.00000000000000  Ge
```

$Ag_2SrSnSe_4$ (*I222*)

(Full HSE06 relaxation geometry based on "tight" basis sets for the lowest-energy structures among 5 space group: *I222, $I\bar{4}2m$, $P3_1$, $P3_2$, Ama2*)

```
lattice_vector  -3.59676838744946   3.82859882236058   4.01727613233262
lattice_vector   3.59676838744946  -3.82859882236058   4.01727613233262
lattice_vector   3.59676838744946   3.82859882236058  -4.01727613233262
atom_frac   0.99411904000000   0.99883983000000   0.99374719000000  Sr
atom_frac   0.49410824000000   0.49891962000000   0.99386661000000  Sn
atom_frac   0.30127448000000   0.80619492000000   0.49375847000000  Ag
atom_frac   0.68648332000000   0.19142904000000   0.49375085000000  Ag
atom_frac   0.48797308000000   0.88663664000000   0.00735040000000  Se
atom_frac   0.86807956000000   0.47899832000000   0.98007998000000  Se
atom_frac   0.50036575000000   0.51890292000000   0.38776168000000  Se
atom_frac   0.11989202000000   0.11110557000000   0.59997990000000  Se
```

$Ag_2BaSnSe_4$ (*I222*)

(Fixed experimental lattice constants with atomic coordinates relaxed by HSE06 based on "tight" basis sets)

```
lattice_vector   -3.55770000000000   3.74970000000000   4.16875000000000
lattice_vector    3.55770000000000  -3.74970000000000   4.16875000000000
lattice_vector    3.55770000000000   3.74970000000000  -4.16875000000000
atom_frac   0.00000000000000   0.00000000000000   0.00000000000000  Ba
atom_frac   0.50002873000000   0.49994152000000   0.00000000000000  Sn
atom_frac   0.68897994000000   0.18942806000000   0.49978030000000  Ag
atom_frac   0.31033658000000   0.81059322000000   0.50004549000000  Ag
atom_frac   0.52361205000000   0.53087046000000   0.40176977000000  Se
atom_frac   0.87096662000000   0.46905004000000   0.99286457000000  Se
atom_frac   0.12896644000000   0.12208775000000   0.59854028000000  Se
atom_frac   0.47680465000000   0.87807799000000   0.00687197000000  Se
```

Cu_2SrGeS_4 (*$P3_2$*)

(Fixed experimental lattice constants with atomic coordinates relaxed by HSE06 based on "tight" basis sets)

```
lattice_vector      5.31999406     -3.07150000      0.00000000
lattice_vector      0.00000000      6.14300000      0.00000000
lattice_vector      0.00000000      0.00000000     15.28200000
atom_frac       0.77956814      0.11304439      0.16649424 Sr
atom_frac       0.88700080      0.66671058      0.49981084 Sr
atom_frac       0.33326621      0.22018407      0.83312187 Sr
atom_frac       0.33341224      0.38205559      0.33312768 Ge
atom_frac       0.61811876      0.95126298      0.66647370 Ge
atom_frac       0.04849853      0.66663861     -0.00019977 Ge
atom_frac       0.25636590      0.25081750      0.58863823 Cu
atom_frac       0.74908646      0.00522871      0.92209713 Cu
atom_frac      -0.00555388      0.74365918      0.25525810 Cu
atom_frac       0.41035075      0.32799466      0.07761719 Cu
atom_frac       0.67245393      0.08313134      0.41090537 Cu
atom_frac       0.91756676      0.58939707      0.74429476 Cu
atom_frac       0.09781069      0.33243427      0.99681779 S
atom_frac       0.66762985      0.76559968      0.33016716 S
atom_frac       0.23458344      0.90195172      0.66347078 S
atom_frac       0.30000400      0.14509301      0.21896560 S
atom_frac       0.85498098      0.15486471      0.55230248 S
atom_frac       0.84486590      0.69979093      0.88562819 S
atom_frac       0.36659311      0.17834313      0.44728020 S
atom_frac       0.82167672      0.18810058      0.78065676 S
atom_frac       0.81162145      0.63352889      0.11395117 S
atom_frac       0.43201526      0.00088234      0.00280293 S
atom_frac       0.99928436      0.43154402      0.33613285 S
atom_frac       0.56881297      0.56772871      0.66947476 S
```

Cu_2BaGeS_4 ($P3_1$)

(Fixed experimental lattice constants with atomic coordinates relaxed by HSE06 based on "tight" basis sets)

```
lattice_vector      5.38234788     -3.10750000      0.00000000
lattice_vector      0.00000000      6.21500000      0.00000000
lattice_vector      0.00000000      0.00000000     15.53400000
atom_frac       0.76855976      0.10198955      0.16832572 Ba
atom_frac       0.89803256      0.66667242      0.50164199 Ba
atom_frac       0.33336187      0.23140033      0.83493128 Ba
atom_frac       0.33327178      0.38008491      0.33500295 Ge
atom_frac       0.62001320      0.95325241      0.66829967 Ge
atom_frac       0.04678574      0.66666041      0.00164171 Ge
atom_frac       0.26061250      0.25118501      0.59104002 Cu
atom_frac       0.74848225      0.00901738      0.92421664 Cu
atom_frac       0.99056321      0.73931346      0.25753347 Cu
atom_frac       0.40593695      0.32420944      0.07908334 Cu
atom_frac       0.67596292      0.08212648      0.41235320 Cu
atom_frac       0.91829903      0.59405905      0.74576773 Cu
atom_frac       0.09591517      0.33589263      0.99858978 S
atom_frac       0.66396440      0.76003464      0.33193081 S
atom_frac       0.24004857      0.90395071      0.66524776 S
atom_frac       0.29302151      0.14391240      0.22179295 S
atom_frac       0.85613305      0.14917146      0.55508993 S
atom_frac       0.85090044      0.70687400      0.88840592 S
atom_frac       0.37359937      0.18425664      0.44823293 S
atom_frac       0.81585442      0.18937883      0.78153071 S
atom_frac       0.81056655      0.62641914      0.11485069 S
atom_frac       0.42665472      0.99742532      0.00469084 S
atom_frac       0.00257410      0.42933347      0.33801768 S
atom_frac       0.57088926      0.57337659      0.67135228 S
```

Cu_2SrSnS_4 ($P3_1$)

(Fixed experimental lattice constants with atomic coordinates relaxed by HSE06 based on "tight" basis sets)

```
lattice_vector      5.44729979     -3.14500000      0.00000000
lattice_vector      0.00000000      6.29000000      0.00000000
lattice_vector      0.00000000      0.00000000     15.57800000
atom_frac       0.33351269      0.37180461      0.33367440 Sn
atom_frac       0.62797873      0.96138324      0.66697325 Sn
atom_frac       0.03880428      0.66693502      0.00029756 Sn
atom_frac       0.77167919      0.10518927      0.16706309 Sr
atom_frac       0.89499230      0.66640722      0.50041901 Sr
atom_frac       0.33326013      0.22842986      0.83366569 Sr
atom_frac       0.26052041      0.24363375      0.58805925 Cu
atom_frac       0.75617480      0.01702920      0.92141647 Cu
atom_frac       0.98297918      0.73887139      0.25461586 Cu
atom_frac       0.40622818      0.31678238      0.07917060 Cu
atom_frac       0.68362856      0.08951350      0.41230274 Cu
atom_frac       0.91004802      0.59400576      0.74578605 Cu
atom_frac       0.09353750      0.31537702      0.00286194 S
atom_frac       0.68512612      0.77811708      0.33621703 S
atom_frac       0.22156141      0.90652776      0.66953463 S
atom_frac       0.29571311      0.11686039      0.21385544 S
atom_frac       0.88304564      0.17847366      0.54716195 S
atom_frac       0.82125543      0.70451923      0.88055812 S
atom_frac       0.37084305      0.15394417      0.45337681 S
atom_frac       0.84550898      0.21657565      0.78670793 S
atom_frac       0.78362082      0.62935095      0.12003215 S
atom_frac       0.44519504      0.01830602     -0.00212353 S
atom_frac       0.98217881      0.42697763      0.33127097 S
atom_frac       0.57274095      0.55485190      0.66450261 S
```

Cu_2BaSnS_4 (*$P3_1$*)

(Fixed experimental lattice constants with atomic coordinates relaxed by HSE06 based on "tight" basis sets)

```
lattice_vector      5.51311772     -3.18300000      0.00000000
lattice_vector      0.00000000      6.36600000      0.00000000
lattice_vector      0.00000000      0.00000000     15.82800000
atom_frac       0.90229786      0.66656149      0.24927990 Ba
atom_frac       0.33342664      0.23567037      0.58259392 Ba
atom_frac       0.76425040      0.09764237      0.91593004 Ba
atom_frac       0.33329993      0.37506759      0.08261632 Sn
atom_frac       0.62487135      0.95819827      0.41594143 Sn
atom_frac       0.04177321      0.66663537      0.74928917 Sn
atom_frac       0.26355770      0.24268310      0.33785242 Cu
atom_frac       0.75723543      0.02080685      0.67117583 Cu
atom_frac       0.97915915      0.73638756      0.00451941 Cu
atom_frac       0.68748056      0.09054144      0.16069681 Cu
atom_frac       0.90940354      0.59689734      0.49404092 Cu
atom_frac       0.40303273      0.31242328      0.82736529 Cu
atom_frac       0.38443522      0.17102270      0.20168308 S
atom_frac       0.82892139      0.21335847      0.53502528 S
atom_frac       0.78658920      0.61551285      0.86835687 S
atom_frac       0.88005084      0.16225793      0.29686393 S
atom_frac       0.83767242      0.71772078      0.63019791 S
atom_frac       0.28224575      0.11987947      0.96352992 S
atom_frac       0.98644194      0.43104623      0.08229276 S
atom_frac       0.56893811      0.55538364      0.41561302 S
atom_frac       0.44458852      0.01351582      0.74894166 S
atom_frac       0.68020770      0.77793195      0.08293055 S
atom_frac       0.22199227      0.90221549      0.41626205 S
atom_frac       0.09771452      0.31974615      0.74959808 S
```

$Cu_2SrGeSe_4$ (*Ama2*)

(Fixed experimental lattice constants with atomic coordinates relaxed by HSE06 based on "tight" basis sets)

```
lattice_vector   3.2705   -5.3675        0
lattice_vector    3.2705   5.3675        0
lattice_vector         0        0   10.807
atom_frac -0.00602832 -0.00602887 1.55e-06 Sr
atom_frac -0.00602318 -0.00602605 0.499999 Sr
atom_frac -0.016793 0.476936 0.577925 Se
atom_frac -0.523068 0.983209 0.422078 Se
atom_frac -0.0167829 0.476934 0.922072 Se
atom_frac -0.523066 0.983216 0.0779261 Se
atom_frac -0.870852 0.337737     0.25 Se
atom_frac -0.662264 0.129148     0.75 Se
atom_frac -0.196099 0.704621 0.249998 Se
atom_frac -0.295381 0.803896 0.750002 Se
atom_frac -0.559414 0.733925     0.25 Ge
atom_frac -0.266076 0.440585 0.750001 Ge
atom_frac -0.197666 0.371901 0.129384 Cu
atom_frac -0.628099 0.802338 0.870614 Cu
atom_frac -0.197675 0.371883 0.370602 Cu
atom_frac -0.628114 0.802326 0.629399 Cu
```

$Cu_2BaGeSe_4$ (*$P3_1$*)

(Fixed experimental lattice constants with atomic coordinates relaxed by HSE06 based on "tight" basis sets)

```
lattice_vector      5.62050487     -3.24500000      0.00000000
lattice_vector      0.00000000      6.49000000      0.00000000
lattice_vector      0.00000000      0.00000000     16.35500000
atom_frac       0.78476517      0.11818246      0.16672568 Ba
atom_frac       0.88182381      0.66659340      0.50005728 Ba
atom_frac       0.33341336      0.21523074      0.83338839 Ba
atom_frac       0.10119354      0.33137298      0.99590016 Se
atom_frac       0.66862918      0.76982861      0.32922268 Se
atom_frac       0.23017684      0.89880765      0.66256591 Se
atom_frac       0.30047116      0.14379960      0.21900900 Se
atom_frac       0.85619883      0.15668667      0.55233962 Se
atom_frac       0.84332756      0.69952523      0.88567393 Se
atom_frac       0.36622005      0.17662178      0.44766054 Se
atom_frac       0.82337603      0.18959383      0.78099570 Se
atom_frac       0.81040485      0.63379328      0.11433025 Se
atom_frac       0.43652339      0.00187518      0.00413011 Se
atom_frac       0.99812516      0.43464984      0.33747009 Se
atom_frac       0.56535062      0.56347699      0.67079604 Se
atom_frac       0.33333997      0.38187935      0.33334256 Ge
atom_frac       0.61812792      0.95146487      0.66667508 Ge
atom_frac       0.04853246      0.66666094      0.00000894 Ge
atom_frac       0.25466123      0.24490314      0.58897378 Cu
atom_frac       0.75508677      0.00974811      0.92230662 Cu
atom_frac       0.99025846      0.74533019      0.25564370 Cu
atom_frac       0.41201381      0.32353699      0.07764531 Cu
atom_frac       0.67644766      0.08845233      0.41097588 Cu
atom_frac       0.91153215      0.58798586      0.74431274 Cu
```

$Cu_2SrSnSe_4$ (*Ama2*)

(Fixed experimental lattice constants with atomic coordinates relaxed by HSE06 based on "tight" basis sets)

```
lattice_vector   3.3475    -5.377        0
lattice_vector    3.3475    5.377        0
lattice_vector         0        0  10.9676
atom_frac -0.810815 0.491253 0.749993 Sn
atom_frac -0.508666 0.189253 0.249989 Sn
atom_frac -0.253161  0.74686 0.500009 Sr
atom_frac  -0.25327 0.746791 -3.898e-05 Sr
atom_frac -0.121374 0.0679109 0.750021 Se
atom_frac -0.932013 0.878679 0.249998 Se
atom_frac -0.420832  0.46298 0.749974 Se
atom_frac -0.536893 0.579278 0.249949 Se
atom_frac -0.758952 0.762971 0.569747 Se
atom_frac -0.236943 0.241257 0.430277 Se
atom_frac -0.758913 0.762947 0.930243 Se
atom_frac  -0.23696 0.241207 0.0697299 Se
atom_frac -0.431322 0.128627 0.631039 Cu
atom_frac -0.871026 0.568763 0.369015 Cu
atom_frac -0.431311 0.128817  0.86907 Cu
atom_frac  -0.87115 0.568804 0.130985 Cu
```

$Cu_2SrSnSe_4$ (*Ama2*)

(Full HSE06 relaxation geometry based on "tight" basis sets)

```
lattice_vector    3.38012704060593  -5.44564688344571   0.00000000000000
lattice_vector   3.38012704060593   5.44564688344571   0.00000000000000
lattice_vector   0.00000000000000   0.00000000000000  11.05482348839839
atom_frac   0.19284046000000   0.49270038000000   0.25007631000000  Sn
atom_frac   0.49263604000000   0.19284399000000   0.75012010000000  Sn
atom_frac   0.74981231000000   0.74988531000000   0.50016820000000  Sr
atom_frac   0.74986598000000   0.74985747000000   0.00000000000000  Sr
atom_frac   0.87760276000000   0.07422264000000   0.25008214000000  Se
atom_frac   0.07416054000000   0.87760938000000   0.75017108000000  Se
atom_frac   0.57672211000000   0.46029389000000   0.25012950000000  Se
atom_frac   0.46016326000000   0.57679248000000   0.75005669000000  Se
atom_frac   0.24359516000000   0.76084589000000   0.43024508000000  Se
atom_frac   0.76075274000000   0.24354870000000   0.57002142000000  Se
atom_frac   0.24367704000000   0.76093011000000   0.07010929000000  Se
atom_frac   0.76081000000000   0.24369377000000   0.93010999000000  Se
atom_frac   0.56824889000000   0.12760188000000   0.36913270000000  Cu
atom_frac   0.12741769000000   0.56817080000000   0.63106975000000  Cu
atom_frac   0.56846279000000   0.12767710000000   0.13106800000000  Cu
atom_frac   0.12757813000000   0.56833496000000   0.86917774000000  Cu
```

$Cu_2BaSnSe_4$ (*Ama2*)

(Fixed experimental lattice constants with atomic coordinates relaxed by HSE06 based on "tight" basis sets)

```
lattice_vector      3.37180000     -5.55525000      0.00000000
lattice_vector      3.37180000      5.55525000      0.00000000
lattice_vector      0.00000000      0.00000000     11.22750000
atom_frac       0.36508847      0.36509717     -0.00027472 Ba
atom_frac       0.36508964      0.36509891      0.49972523 Ba
atom_frac       0.92214180      0.62485080      0.24971885 Sn
atom_frac       0.62484303      0.92215229      0.74973194 Sn
atom_frac       0.87137215      0.36389971      0.07084888 Se
atom_frac       0.36389039      0.87137994      0.92860168 Se
atom_frac       0.87137110      0.36389354      0.42860339 Se
atom_frac       0.36388436      0.87137985      0.57084736 Se
atom_frac       0.55317781      0.67334360      0.24972654 Se
atom_frac       0.67333481      0.55318641      0.74972419 Se
atom_frac       0.25108128      0.03432707      0.24972636 Se
atom_frac       0.03431670      0.25108898      0.74972409 Se
atom_frac       0.55536039      0.98969194      0.12889074 Cu
atom_frac       0.98968299      0.55536759      0.87055964 Cu
atom_frac       0.55535297      0.98968571      0.37056358 Cu
atom_frac       0.98967657      0.55536209      0.62888712 Cu
```

Cu_2ZnSnS_4 ($I\bar{4}$)
(Full HSE06 relaxation geometry based on "tight" basis sets)

```
lattice_vector      5.45364782     -0.00083923     -0.00085441
lattice_vector      0.00197489      5.45429115     -0.00026046
lattice_vector      0.00087251     -0.00004896     10.87562125
atom_frac      -0.00033648     -0.00036581      0.50013299 Sn
atom_frac       0.49967745      0.49965478      0.00011399 Sn
atom_frac      -0.00038257     -0.00037037      0.00011723 Cu
atom_frac       0.49966605      0.49964598      0.50017300 Cu
atom_frac      -0.00029711      0.49960639      0.25013397 Cu
atom_frac       0.49957616     -0.00036418      0.75013033 Cu
atom_frac      -0.00033440      0.49962260      0.75011897 Zn
atom_frac       0.49963903     -0.00032992      0.25010389 Zn
atom_frac       0.24122913      0.24418130      0.12829961 S
atom_frac       0.75810941      0.75511657      0.12832538 S
atom_frac       0.24415675      0.75807662      0.87188135 S
atom_frac       0.75515464      0.24120816      0.87186916 S
atom_frac       0.74122064      0.74416635      0.62833002 S
atom_frac       0.25812926      0.25515254      0.62831601 S
atom_frac       0.74418643      0.25808282      0.37187081 S
atom_frac       0.25517101      0.74123643      0.37187172 S
```

▪ REFERENCES

(1) Blum, V.; Gehrke, R.; Hanke, F.; Havu, P.; Havu, V.; Ren, X.; Reuter, K.; Scheffler, M. Ab Initio Molecular Simulations with Numeric Atom-Centered Orbitals. *Comput. Phys. Commun.* **2009**, *180*, 2175–2196.
(2) Hersh, P. A. Wide Band Gap Semiconductors and Insulators: Synthesis, Processing and Characterization, Oregon State University, USA, 2008.
(3) Setyawan, W.; Curtarolo, S. High-Throughput Electronic Band Structure Calculations: Challenges and Tools. *Comput. Mater. Sci.* **2010**, *49*, 299–312.
(4) AFLOW-online http://aflowlib.org/aflow_online.html.
(5) Tampier, M.; Johrendt, D. Kristallstrukturen Und Chemische Bindung von AM_2GeSe_4 (A = Sr, Ba; M = Cu, Ag). *Zeitschrift für Anorg. und Allg. Chemie* **2001**, *627*, 312–320.